Radiocarbon, Vol 58, Nr 3, 2016, p 583–598 DOI:10.1017/RDC.2016.40

USE OF LIGHTWEIGHT LIME MORTAR IN THE CONSTRUCTION OF THE WEST CHURCH OF UMM EL-JIMAL, JORDAN: RADIOCARBON DATING AND CHARACTERIZATION

Khaled Al-Bashaireh*

Department of Archaeology, Yarmouk University, postal code 211-63, Irbid, Jordan.

ABSTRACT. Lightweight concrete was widely used and mainly spread during the Roman period. This technology was used in the West Church, Umm el-Jimal, Jordan. The date of construction of the West Church is debated and different dates have been suggested based on its architectural styles and comparisons with other churches. This research aims to radiocarbon date the construction of the dome (church), archaeometrically characterize the mortar, and determine the source of the scoria. Three charcoals and two broken pieces comprising scoria from the mortar of the fallen dome and six large scoria samples from Quais cone were collected. The research used different analytical methods including accelerator mass spectrometry ^{14}C, X-ray diffraction, petrographic microscopy, inductively coupled plasma mass spectrometry, and scanning electron microscopy-energy dispersive X-ray spectroscopy. ^{14}C determinations dated the dome (church) to the Late Roman–Early Byzantine periods, which contradicted the archaeological data. Analytical results showed that the mortar is lime-based and hydraulic. The similarities in the mineralogical composition, macroscopic and microscopic features, and chemical composition (compared statistically) of the scoria samples and the short distance between Umm el-Jimal and the Quais volcanic cone very likely indicate that the Quais volcanic cone is the source of the scoria used in the fallen dome.

KEYWORDS: radiocarbon, lightweight concrete, West Church, Umm el-Jimal, Jordan.

INTRODUCTION AND HISTORIC BACKGROUND

The wide use of mortar (concrete) vaulting to create large open rooms and covered passageways during the Roman period resulted from the ability of the Roman builders to regulate the weights of the vaults' components (Letchman and Hobbs 1987). Therefore, lightweight volcanic rocks such as scoria and pumice were employed to construct vaults aiming at reducing their weight, and consequently reducing the lateral forces on the supporting walls and controlling the forces within the structures (Lancaster et al. 2011). The great Roman Pantheon temple and the Colosseum amphitheater are examples of spectacular structures of Roman vaulting that still exist in Rome. They were built about 2000 yr ago using a concrete composed of lightweight aggregates. The principal contribution of the Byzantines to vaulting is the dome of the Hagia Sofia cathedral (Istanbul, Turkey), which was built in the 6th century AD using similar materials as used by the Romans (Sebestyén 1998; Chandra and Berntsson 2002). After the 2nd century AD, this building technique spread throughout the Roman Empire, usually to areas that had lightweight volcanic rocks readily available, while areas that lacked these materials imported them [see Lancaster et al. (2010) for the diffusion of this technique into Turkey and Tunisia].

Both scoria and pumice are vesicular volcanic lightweight rocks. Compared to pumice, scoria usually has larger and more regular vesicles, greater specific gravity, is darker in color, and contains more iron (Fe) and magnesium (Mg) and less silica (SiO_2) (Hossain 2006; Kwon et al. 2010). Scoria is a pyroclastic rock of a basaltic to andesitic composition with a vesicular texture; therefore, it is light in weight but with a specific gravity normally greater than 1. Due to its iron content, it varies in color from black to reddish brown. Scoria may form fragments or steep-sided cones as part of a lava flow (Kogel 2006). In ancient times, scoria was widely utilized in the manufacturing of lightweight concrete (Lancaster 2011).

In northeast Jordan, scoria was used as fine-grained aggregates in the production of pozzalanic lime mortars (Dunn and Rapp 2004) and large fragments in lightweight mortar (concrete)

*Corresponding author. Email: khaledsm@email.arizona.edu.

Figure 1 *In situ* parts of the fallen dome of the West Church

(Butler 1913) for building Umm el-Jimal's structures. The dome of the West Church represents an example of this technology. *In situ* parts of the fallen half dome of the semi-circular apse are made of scoria-based lightweight mortar (Figure 1). Cones of scoria are spread throughout the northeastern part of Jordan and southern parts of Syria within the Harratt Ashaam volcanic field (Bender 1974). Harrat Ajjabban (the part of Harrat Ashaam located in Jordan) comprises (among others) the Remah, Hassan, Quais, and Fahem cones. The closest volcanic cone to Umm el-Jimal is Quais.

Umm el-Jimal (Figure 2) belongs to the southern Hauran region, which is covered by basalt flows. The structures of the site were built with this black stone. The Nabateans (who founded Umm el-Jimal in the 1st century AD), Romans, Byzantines, and Umayyads (2nd–8th centuries AD) established many military, civil, and religious structures (mainly churches) and made it a farming and trade center (for more details see De Vries 1993, 1994, 1998; Al-Bashaireh 2014).

THE WEST CHURCH

The West Church, named for its location, is located just outside the west wall of the city near the gate of Commodus, but it remained connected to the Roman gate and the city wall north of the Praetorium by two walls (Butler 1913). It is described as a funerary church because of the presence of an underground mausoleum and sarcophagus outside the narthex. The church has a nave and two aisles, where each aisle is separated from the nave by four arches. It has an arched narthex between two square towers. Some of the arches are ornamented with carved discs containing Christian crosses and other emblems. The two aisles were roofed with flat stone slabs resting upon the aisle walls and a corbel course above the arches of the nave (Butler 1913). The floor of the church was paved with mosaic work of geometrical patterns in various bright colors (Butler 1913). Careful examination of the mosaic floor showed two mosaic layers, which might indicate a restoration stage of the church's floor. The two stories at the church's west end and a clearstory wall above the south arcade of the aisle are quite well preserved (Figure 3).

Owing to the absence of inscriptions, the age of the church is unknown and scholars have debated its construction date. The classical moulding that divides the stories of the façade and the quadrated stones suggest that they originated from abandoned Roman buildings

https://doi.org/10.1017/RDC.2016.40 Published online by Cambridge University Press

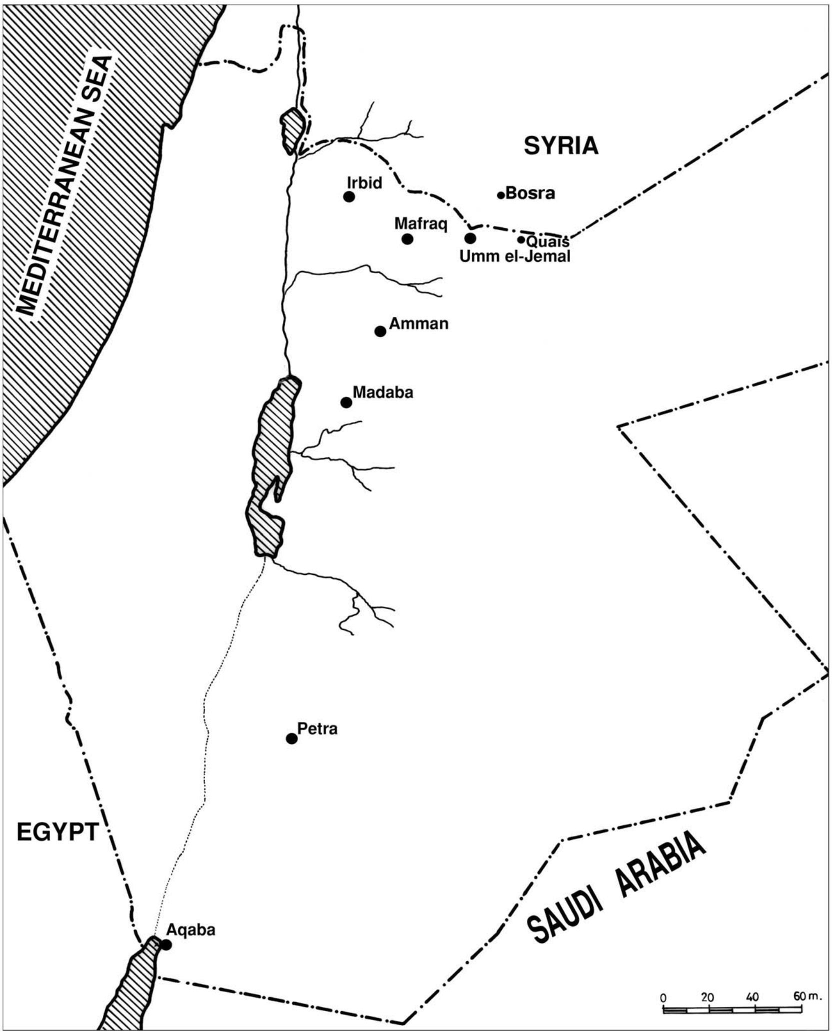

Figure 2 Location map of Umm el-Jimal

(Butler 1913) or were a direct Roman architectural influence in the construction of the church. De Vries (1990) did not give a specific date for the church's construction but suggested a relatively late date based on its location and poor construction. However, Butler (1913) stated that the church was apparently the most beautiful of Umm el-Jimal churches and that the church's plan and construction methods are different from the churches of southern Syria (Hauran) and matches those of northern Syria. In addition, Butler (1913: 115) considered the West Church as one of the 6th century churches that were classified into three classes, categorizing it as the Class I type (the Basilica type with longitudinal supports composed of piers or columns and arches).

This church is characterized by having a semicircular apse roofed with a half dome and lined by two large rooms. The apse of the church was partitioned into a room after the building lost its function as a church (De Vries 1990: 31). The church is constructed with smooth quadrated basalt,

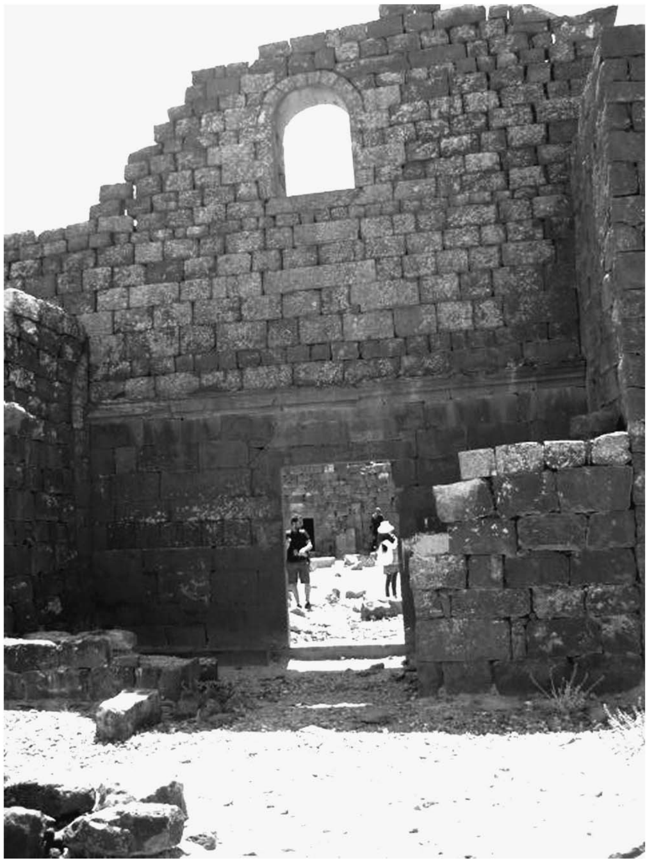

Figure 3 The west entrance of the west church

while the half dome of the apse is built with a scoria lightweight mortar. It is worth mentioning that the crown of the half dome has fallen; two large blocks of the mortar are still *in situ* (Figure 1), while the rest of the mortar can be seen near the north and south walls of the church.

Figure 4 Quais volcanic cone facing south

https://doi.org/10.1017/RDC.2016.40 Published online by Cambridge University Press

QUAIS VOLCANIC CONE

The main source of scoria in the area is the volcanic cones spread throughout Jordan and south Syria. The closest volcano cone to Umm el-Jimal is Quais, which is located about 25 km east of Umm el-Jimal at 32°19′24″N and 36°38′33″E (see Figure 2). It has a depression forming a crater and a height of about 60 m (Figure 4).

Quais is mainly composed of uniform bedded lapilli (0.8–14 mm) of scoria, which shows limited vertical and horizontal variations and a symmetrical cone shape sloping 20° inwards and outwards (Al-Malabeh 1993: 44–5). The scoria is compacted but friable and varies in color from gray to black in the upper part of the cone and from reddish-brown to dark brown in its lower part.

MATERIALS AND METHODS

Radiocarbon Dating

Three charcoals were collected from different parts of the *in situ* mortar for ^{14}C dating. The chosen charcoals were rounded and of small diameter; therefore, it is very likely they belong to short-lived twigs, shrubs, or tree stems. The ^{14}C dates, in this case, will overcome the problem of old wood (see Bowman 1990). Charcoal samples were acid-base-acid (ABA) pretreated and dated at the Arizona NSF Accelerator Mass Spectrometer Laboratory in Tucson, USA (Jull et al. 2004). Initially, they were soaked in diluted (1N) hydrochloric acid and rinsed with distilled water, then soaked in diluted (0.1%) sodium hydroxide and rinsed with distilled water. Next, samples were soaked in acid and rinsed with distilled water until the washing water is neutral. After drying, a few milligrams of the cleaned charcoal were converted into carbon dioxide by combusting them at about 900°C in a chemistry (combustion) line with copper oxide (CuO). The gas collected was graphitized using iron as a catalyst and zinc as a reducing agent. Finally, graphite powders were AMS ^{14}C dated. Date calibration was accomplished using the OxCal software v 4.2 (Bronk Ramsey 2009; Bronk Ramsey and Lee 2013) and the IntCal13 (Reimer et al. 2013) data. Calibrated ages are presented at the 68.2% and 95.4% confidence intervals.

Mortar Characterization

Two large broken concrete samples (Samples 6 and 8) comprising cement material (a binder) and scoria were collected from two different parts of the fallen dome, and six scoria samples (1, 2, 3, 4, 5, 7) were collected from different levels of the Quais scoria cone. Powders from the binders of the two concretes were collected for X-ray diffraction (XRD) analyses. Two small chips comprising the binder and scoria were cut off from the two concretes for scanning electron microscopy-energy dispersive X-ray spectrometry (SEM-EDX) analyses and thin-section preparation. Small parts from the scoria comprising in the two concretes and the six scoria samples from Quais were removed, then cleaned and divided into two pieces. The first piece was used for thin-section preparation and the second was crushed and finely ground in an agate mortar for XRD and inductively coupled plasma mass spectrometry (ICP-MS) analyses.

Thin-section petrographic analyses of the concretes were carried out to identify the various aggregates and organic inclusions present and their grain-size distribution, binder/aggregate ratio, etc., while petrographic analyses of scoria samples identified their mineralogical composition and textures. To prepare a thin section, the chips were solidified by impregnating them under vacuum with a low-viscosity resin (Camuti and McGuire 1999). The hardened block was carefully polished until the resulting thin section was about 0.03 µm thick. Thin sections were prepared and examined using a Leitz (7062 model) polarized light microscope.

XRD analyses of the powders of the binders and scoria were used to determine their mineralogical composition. XRD analyses were obtained on powders using a Shimadzu Lab X, 6000 X-ray diffractometer under the following conditions: 2Θ from 10–70°, CuK∝ radiation (1.5418A°) with 30 kV, 30 mA energy and graphite monochromatic. Thin-section and XRD analyses were performed at the Archaeometry Laboratory of the Faculty of Archaeology and Anthropology at Yarmouk University in Irbid, Jordan.

SEM was used to show the growth of the binder particles and their interaction with the aggregates. Semi-quantitative analysis was performed by SEM-EDX to define the chemical composition and hydraulic properties of the concrete. Analyses were performed using an FEI Quanta 200 scanning electron microscope equipped with an EDS (Energy Dispersive X-ray Microanalyzer) at the SEM laboratory, Department of Earth and Environmental Sciences, Faculty of Science, Yarmouk University. Fresh fractures of small pieces of bulk samples were coated with a thin layer of gold and analyzed under the following conditions: run at an accelerating voltage between 0.3 and 30 kV, with the chamber's pressure about 50 Pa in a variable-pressure mode.

ICP-MS was used to determine the major and trace elements of the scoria samples. The data collected from the two scoria samples from the lightweight mortar were compared to those from the six scoria samples from the Quais cone. Furthermore, the results were compared to those collected by Al-Malabeh (1993), who studied Quais and three other volcanic cones (Remah, Fahem, and Hassan), although the latter were more distant than Quais from Umm el-Jimal. The samples were chemically prepared by the following procedure: 0.25 g was accurately taken from the powder of each sample, 2 mL of concentrated hydrofluoric acid (HF analytical grade 48%), 8 mL of concentrated HNO_3 (analytical grade 65%), and 2 mL of H_2O_2 (hydrogen peroxide 30%) were added to the samples and digested using a Milestone ETHOS1 microwave digestion system. Subsequently, the samples were transferred volumetrically to a 50-mL centrifuge test-tube at room temperature, treated with 4% boric acid to eliminate the excess of HF, centrifuged by a NF 1200 centrifuge system, and diluted to 50 mL as a last step in the primary chemical preparation. They were then additionally diluted with 1% subboiled distilled nitric acid (HNO_3 65%) by a factor of 2000, 100, and 50 times depending on the element measured.

Analyses were performed using an ICP Bruker 810/820-ICP mass spectrometer. Five calibration standards of the AccuTrace reference standard were prepared for all the measured elements. A blank was also prepared in 1% subboil nitric acid 65% (HNO_3) solution. Yttrium (Y) was used as an internal standard for Al, Ca, Fe, K, Mg, Na, P, and Si correction measurements; indium (In) and terbium (Tb) were used as internal standard for Ba, Cr, Cu, Mn, Mo, Ni, Pb, Sr, Th, Ti, U, V and Zn correction measurements; and In was used for Dy, Er, Eu, Gd, Hf, Ho, La, Lu, Nb, Nd, Pr, Rb, Sm, Ta, Tb, Y, Yb, and Ce correction. Millipore high-quality water >18 Ωι ohm was used in all steps of the preparation procedure. Wet chemical techniques were used to measure the loss on ignition (LOI). The internal standards were added to all samples, calibration standards, matrix blank, duplicate samples, and the certified reference material. The matrix blank, duplicate sample, and certified reference material were analyzed together with the samples as part of the quality control process. The results for the certified reference material are within the expected reference values excluding Si. The measured values were better than 5% for Sm, Tb, Er, Eu, Ho, Nb, Dy, and Ca; between 5 and 10% for B, Al, and Ti; between 10 and 15% for Mn, Fe, P, Na, Ce, Zn, V, U, Th, Sr, Pb, Cu, Cr, Nd, La, Gd, Yb, and Pr; between 15 and 20% for Y, Yb, and Lu; between 20 and 25% for Rb, Mg, and K; and between 25 and 30%

for Ni. The ICP analysis was performed at the laboratories of Research Laboratories and Information Directorate, Jordan Atomic Energy Commission JAEC, Amman.

RESULTS AND DISCUSSION

Radiocarbon Dating

Table 1 and Figure 5 (a,b,c) present the ^{14}C determinations obtained from the three charcoals collected from different parts of the fallen dome.

Initially, one charcoal was dated and gave an age range between AD 138 and 380 at 95.4% probability. Although 23.14% of this age period comprises an early 56-yr part of the Byzantine

Table 1 Radiocarbon determinations of the charcoal samples.

					Calendar age AD	
Lab code	Material	δ^{13}C (‰)	F(δ^{13}C) ± *df*	^{14}C date ± SD	68.2%	95.4%
AA-96289	Charcoal	–14.9	0.8026 ± 0.0036	1766 ± 36	231–333	138–380
AA-103285	Charcoal	–27.0	0.8013 ± 0.0046	1779 ± 46	171–333	130–380
AA-106918	Charcoal	–11.1	0.8004 ± 0.0021	1789 ± 21	178–321	138–326
		Combined date = 1783 ± 17				143–329

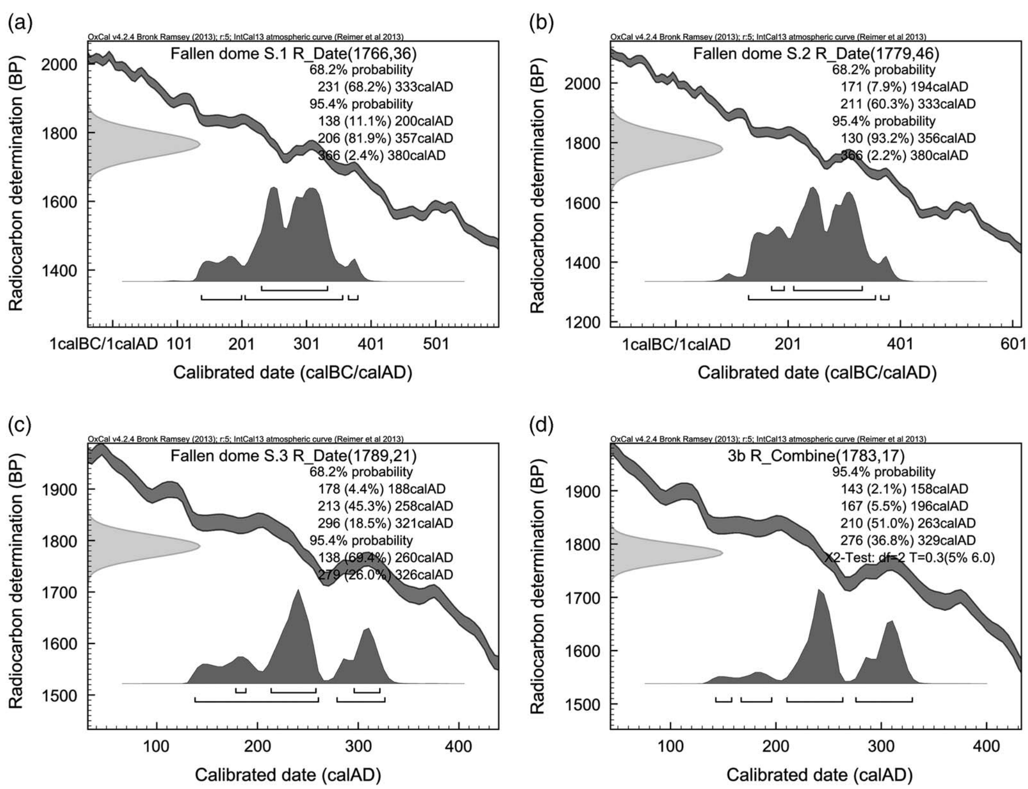

Figure 5 (a, b, c) Calibrations for the ^{14}C dates and (d) the calibration for the combined ^{14}C date

https://doi.org/10.1017/RDC.2016.40 Published online by Cambridge University Press

period (AD 324–636), 76.86% of the age period falls in the Roman period (63 BC–AD 324). It was suspected that the charcoal might present an older age than the real age because of the old-wood effect; thus, a second charcoal sample was ^{14}C dated. The second determination ranged between AD 130 and 380 (at 95.4%), which confirmed and coincided with the first one. In addition, a third charcoal was dated to reconfirm these two results, and the new ^{14}C determination gave a more precise date for the dome (AD 138–326). The combined date of the three determinations suggests an age between AD 143–329 (Table 1, Figure 5d). This date fully assigns the dome (and thus the church) to the late Roman period.

All three determinations suggest an age for the construction of the dome older than the archaeological record. Although the Christian community started to grow in Jordan before the 4th century (such as in Pella), most probably, the dome of the church was constructed in the 4th century AD or during the early years of the Byzantine period. Umm el-Jimal belonged to the Bosra Bishopric (Piccirillo 1981). During the Byzantine period, Bostra was an important religious capital and became a center for the episcopal chair after the spread of Christianity. For example, Bosra's bishops participated in the Council of Antioch. The close distance between Umm el-Jimal and Bosra, the legalization of Christianity and its spread in the region under the patronage of the 4th century emperors, and the foundation of Constantinople (Istanbul, the capital of the Eastern Roman Empire) (Watson 2001) are suggested reasons for the construction of the church in the 4th century AD. It is not unusual that the church is dated to the 4th century AD because Umm el-Jimal has another church of the same age. The church of Julianos (dated to AD 345) is one of the earliest dated churches in all Syria and Jordan (Butler 1913).

Mortar Characterization

Technology of the Lightweight Mortar Used in the Fallen Dome

XRD and SEM analyses showed that the binder of the mortar used in the construction of the fallen dome is lime-based (Figure 7a,b). Petrographic analyses showed the presence of basalt, grog, mortar remnants, and charcoals added to the lime binder (Figure 6). Aggregates are

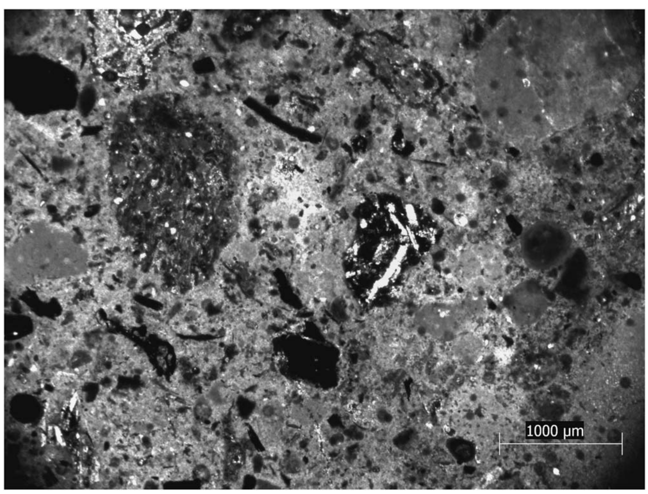

Figure 6 Ashy lime-based mortar of the fallen dome with aggregates of basalt, grog, and charcoal.

commonly added in different sizes to increase the cohesion and adhesion forces of the mixture and to improve its strength, durability, and workability (Moropoulou et al. 2000; Stefanidou and Papayianni 2005). As mentioned previously, the source of the scoria is likely one of the volcanic cones in the area. Because the closest cone to Umm el-Jimal is Quais, it is probable that the Umm el-Jimal stonemasons quarried the scoria from it. This hypothesis is examined in further detail in the following.

Hydraulicity of the Mortar

The addition of scoria particles caused an increase in calcium, aluminum, and iron silicates in the binder of concrete samples as shown by the SEM-EDX analyses of the binder (lime-cement) (Figure 7a,b), scoria (Figure 7c,d), and interaction layer between them (Figure 7e,f). It is known that quicklime is a nonhydraulic compound, but slaked lime can attain hydraulic properties and more strength when mixed with natural or artificial pozzolanic materials, in this case scoria, and harden with the addition and/or under water (Harries 1995). Scoria contains silicates and aluminates that react, in the presence of water, with the slaked lime to form new compounds of cementitious properties (Moropoulou et al. 1995, 2004; Duran et al. 2008).

Source of the Scoria

The source of the scoria samples used in the construction of the fallen dome was determined in this research by comparing the macroscopic, microscopic, mineralogical, and chemical characteristics of the scoria samples from the dome to those from the Quais volcanic cone.

1. Macroscopic Examination

Macroscopic examination of the samples showed that the scoria samples of the dome are similar to these collected from the Quais volcanic cone. The scoria samples are black to blackish-gray or brownish red when fresh and deep brown or yellowish-brown when weathered. They have basaltic compositions with vesicles, about 60% of the material mass and up to 7 mm in size. Some of the vesicles are interconnected and with common shapes being spherical, subspherical, and ovoid (see Figure 8). In some altered scoria, the vesicles are filled with secondary minerals including carbonates, quartz, and possibly zeolites.

2. Petrographic Analysis

The studied samples are scoraceous extrusive rocks of similar features. Most of the vesicles are empty, while some others are partially filled with secondary calcite, forming an amygdaloidal texture. In general, the percentages of vesicles or pore spaces range between 50 and 70% and are badly sorted, rounded to subrounded to oval in shape, and sometimes are connected. The samples show porpheritic and hypocrystalline textures and are mainly characterized by the presence of phenocrysts of certain minerals (plagioclase, olivine, and/or pyroxene) in hyaline and fine-grained plagioclases in the groundmass (Figure 8); however, the amounts of these minerals differ from one sample to another. The main products of the chemical alteration of olivine phenocrysts of weathered samples (except the fresh Samples 3 and 4) are iddingsite, distinguished by its red blood color, and/or opaque iron oxides (hematite).

3. XRD Analysis

XRD analysis show a similarity between the mineralogical compositions of all the samples (Figure 9) and confirm the results obtained by petrographic analysis that the samples are mainly composed of plagioclase, olivine, pyroxene, and hematite (iron oxide).

https://doi.org/10.1017/RDC.2016.40 Published online by Cambridge University Press

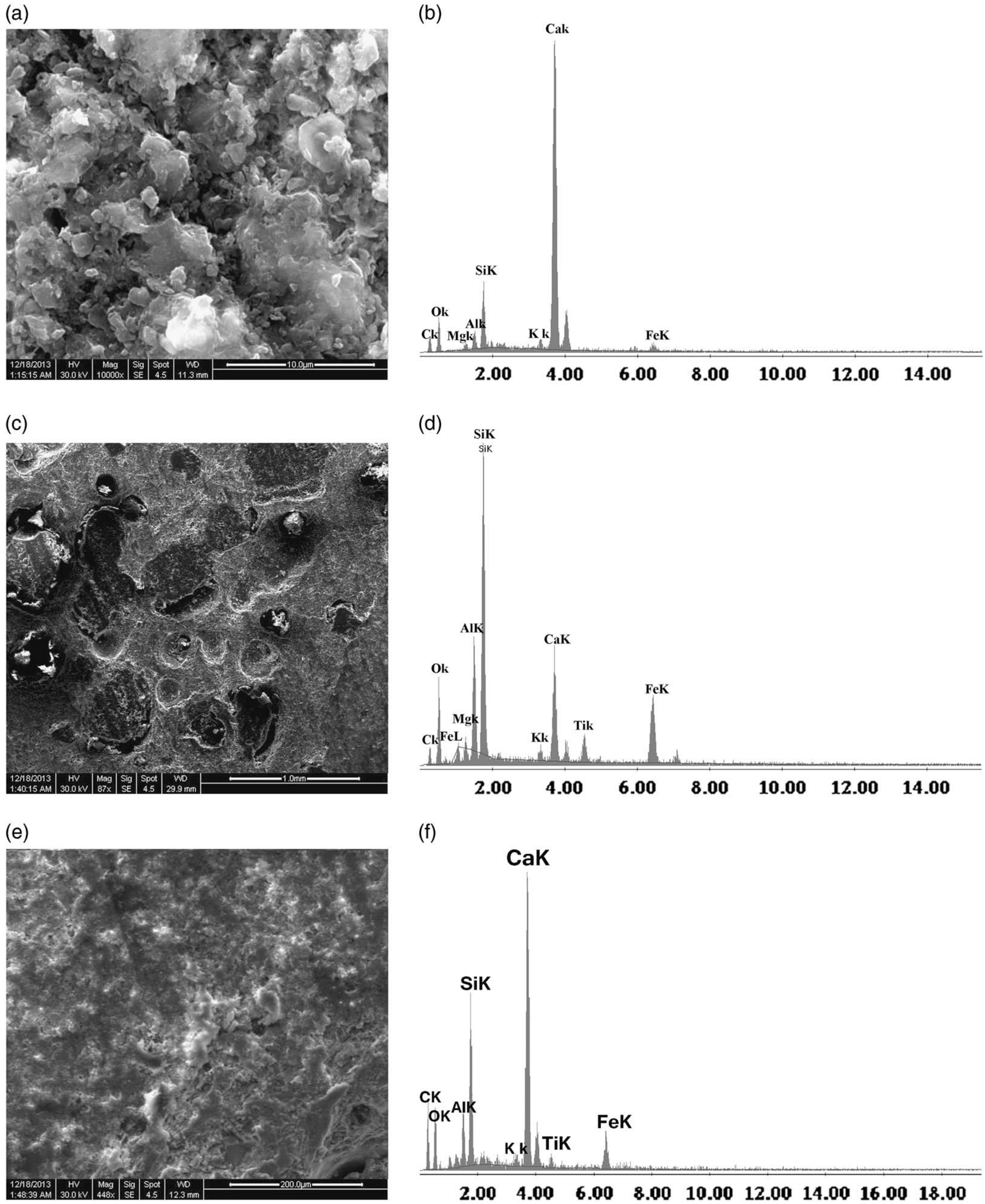

Figure 7 Hydraulic composition of the mortar (e,f), which is formed from the reaction between the mortar (a,b) and scoria (c,d).

4. Chemical Analysis

The results of the major and minor oxide anlyses are presented in Table 2 while the trace element analyses are presented in Table 3. The high values of loss on ignition (LOI) of Samples 2, 7, and 8 in Table 2 indicate weathering and alteration, while the remaining samples have an LOI less than 1.7, indicating fresh samples. Therefore, standard classification based on major

https://doi.org/10.1017/RDC.2016.40 Published online by Cambridge University Press

(a)

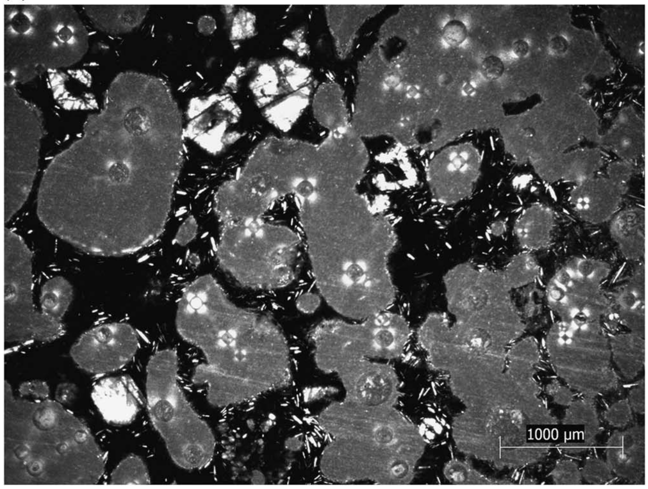

(b)

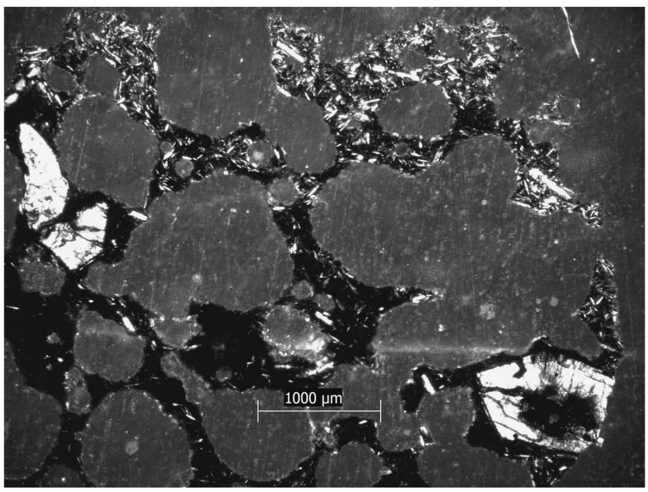

Figure 8 Scoraceous structure of a phorpheritic texture of Samples 4 (a) and 8 (b) (olivine, pyroxene, and plagioclase laths in a fine plagioclase laths).

oxides (such as SiO_2, Na_2O, K_2O, CaO) cannot be used for altered and/or contaminated volcanic rocks (Lancaster et al. 2011). On the contrary, the concentrations of other elements such as yttrium and niobium do not vary because of weathering and/or low-metamorphism processes. Their measured values are close to each other in most of the samples and are similar to the values reported by Al-Malabeh (2013). However, a visual comparison between the results of the scoria samples from the fallen dome and those from the Quais cone shows similar chemical compositions of various elements. This observation was examined statistically by the Statistical Package for the Social Sciences (SPSS) (Sweet and Grace-Martin 2012) using the analysis of variance (ANOVA) method. The ANOVA test in Table 4 at a level of significance of 0.05 ($\alpha = 0.05$) shows that there is no significant difference between all the samples since the significance (p value $= 0.968$) is greater than α (0.05). The Scheffe test (Table 5) was used to compare Samples 6 and 8 with the rest of the samples and showed no significant difference between them.

https://doi.org/10.1017/RDC.2016.40 Published online by Cambridge University Press

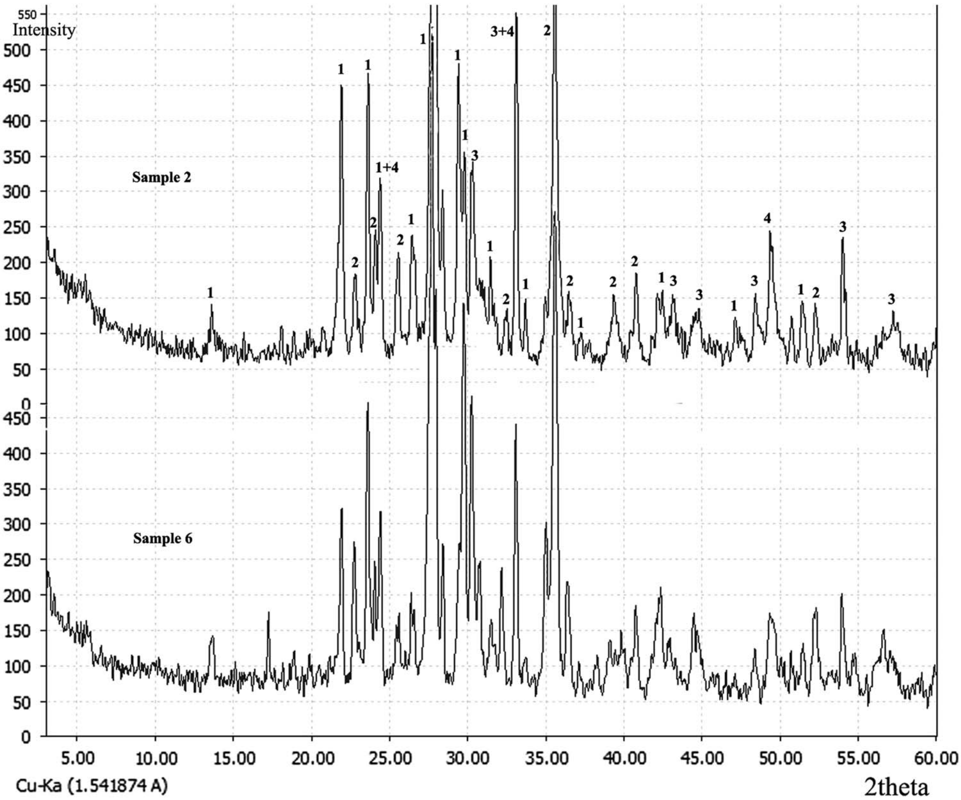

Figure 9 Similarity between XRD analyses of scoria Samples 2 and 6 (1 = plagioclase, 2 = olivine, 3 = pyroxene, 4 = hematite).

Table 2 Major and minor oxides of the scoria samples (oxides in wt%, CRM reference in PPM)

Sample	Na_2O	MgO	Al_2O_3	SiO_2	K_2O	P_2O_5	CaO	Fe_2O_3 total	FeO	TiO_2	MnO	LOI
1	3.30	8.60	13.00	39.0	1.30	1.00	6.30	13.30	6.00	2.30	0.20	0.5
2	2.50	6.40	13.50	44.5	0.50	0.20	9.70	12.50	5.60	1.90	0.20	4.9
3	3.10	8.30	12.80	39.3	1.30	0.70	8.90	13.30	6.00	2.40	0.20	0.5
4	3.00	8.20	13.00	39.7	1.10	0.00	6.60	13.60	6.10	2.40	0.20	1.2
5	3.00	8.40	13.30	39.3	1.30	0.50	7.40	13.40	6.00	2.30	0.20	1.7
6	3.30	8.30	13.70	42.7	1.40	0.50	7.30	13.70	6.10	2.30	0.20	1.7
7	2.40	7.50	13.60	42.4	1.40	0.80	8.30	10.90	4.90	1.80	0.20	5.1
8	3.00	8.80	13.60	39.8	1.20	0.90	12.20	12.30	5.50	2.10	0.20	3.2
CRM-U-ORE given	0.49	1.60	1.94	5.90	0.70	0.88	28.05	1.47	1.32	0.105	0.01	
CRM-U-ORE measured	0.56	1.22	1.77	3.20	0.53	1.04	29.42	1.25	1.13	0.113	0.01	

Furthermore, the Kruskal-Wallis test was used at $\alpha = 0.05$ to support these results because the samples are not normally distributed as shown in Table 6. The Kruskal-Wallis test results in Table 7 confirm the earlier results that showed no significant differences present between Samples 6 and 8 and the other samples.

https://doi.org/10.1017/RDC.2016.40 Published online by Cambridge University Press

Table 3 Trace elements analysis of the scoria samples (all values are in PPM).

Sample	Ba	Cr	Cu	Ni	Pb	Sr	Th	U	V	Zn
1	274.1	2751.6	159.0	1389.5	57.4	683.5	5.3	1.0	191.5	141.8
2	208.4	3476.2	91.7	1762.0	82.6	458.7	3.2	0.8	168.9	123.2
3	286.2	2493.9	157.4	1294.4	56.9	710.8	3.8	1.1	195.7	149.4
4	289.1	2984.8	94.0	1515.7	8.60	684.4	3.9	1.1	197.1	140.0
5	278.7	2447.6	74.5	1261.0	111.6	683.1	3.8	1.2	185.7	147.90
6	270.2	2873.9	147.6	1440.8	263.9	635.6	3.7	1.0	152.5	137.1
7	211.0	663.4	102.5	477.0	6.5	451.7	3.4	0.9	188.1	132.9
8	254.0	216.6	84.9	291.6	3.0	517.1	2.6	0.5	187.1	115.6
CRM-U-ORE Given	635.32	208.00	93.00	253.00	4.9	771.00	2.5	423	616.00	484.00
CRM-U-ORE Measured	592.32	185.75	75.10	320.90	4.19	685.25	2.14	371.32	536.53	532.67

Sample	Ce	Dy	Dy163	Er166	Er167	Eu151	Eu153	Gd155	Gd157	Yb171	Yb172	Yb173	Ho165	La139
1	50.9	4.2	4.2	1.9	1.9	2.0	2.0	7.1	5.5	1.3	1.3	1.3	0.7	24.3
2	33.5	3.8	3.8	1.9	1.89	1.4	1.4	5.3	4.3	1.5	1.5	1.5	0.7	15.5
3	52.9	4.3	4.3	1.9	1.8	2.0	1.7	7.2	5.6	1.3	1.4	1.3	0.7	25.4
4	50.9	4.1	4.3	1.9	1.8	1.9	1.9	6.9	5.4	1.3	1.4	1.3	0.7	24.3
5	51.8	4.1	4.2	1.9	1.8	1.9	1.9	6.9	5.3	1.3	1.3	1.3	0.7	24.8
6	46.5	4.1	4.1	1.9	1.9	1.8	1.7	6.4	5.1	1.4	1.4	1.4	0.7	22.6
7	35.2	3.6	3.6	1.8	1.8	1.4	1.3	5.2	4.2	1.4	1.4	1.3	0.6	16.3
8	36.8	3.6	3.6	1.9	1.8	1.5	1.5	5.5	4.2	1.3	1.3	1.3	0.7	17.9
CRM-012-JAEC Given	37.6	4.6	4.6	2.2	2.2	1.60	1.60	5.30	5.30	1.83	1.83	1.83	0.80	17.4
CRM-012-JAEC Measured	30.88	4.39	4.42	2.16	2.11	1.56	1.54	5.98	4.71	1.53	1.56	1.54	0.80	14.79

Sample	Lu175	Nb93	Nd143	Nd145	Nd146	Pr141	Rb85	Sm147	Sm149	Ta181	Tb159	Y89
1	0.2	40.4	26.2	27.1	26.8	6.3	17.9	6.0	5.9	3.5	0.8	16.3
2	0.2	26.2	17.8	18.5	18.3	4.2	11.5	4.3	4.3	1.8	0.7	16.6
3	0.2	43.5	26.9	28.1	27.7	6.5	19.4	6.2	6.0	2.9	0.8	17.7
4	0.2	42.0	25.7	26.6	26.3	6.3	17.1	5.8	5.6	2.7	0.8	17.5
5	0.2	43.2	26.0	26.6	26.4	6.3	18.7	5.8	5.8	2.6	0.8	18.3
6	0.2	42.0	23.3	23.9	23.7	5.8	16.6	5.4	5.3	2.5	0.7	18.7
7	0.2	25.3	18.0	18.5	18.3	4.3	18.8	4.4	4.2	1.6	0.6	17.2
8	0.2	36.5	18.5	19.0	18.8	4.5	8.6	4.3	4.2	2.1	0.6	17.2
CRM-012-JAEC Given	0.20	21.00	19.90	19.90	19.90	4.70	22.40	4.70	4.70	—	0.81	22.9
CRM-012-JAEC Measured	0.24	21.32	17.15	17.82	17.67	4.00	17.64	4.54	4.58	1.69	0.82	18.38

Table 4 Analysis of variance (ANOVA) test.

	Sum of squares	Degrees of freedom (*df*)	Mean square	*F* value	Significance (*p* value)
Between samples	277405.239	7	39629.320	0.263	0.968
Within samples	50610620.843	336	150626.848		
Total	50888026.083	343			

Table 5 Scheffe multiple comparison test.

					95% confidence interval	
I samples	*J* samples	Mean difference (*I–J*)	Standard error	Significance	Lower bound	Upper bound
Sample 6	Sample 1	4.825279	83.701254	1.000	–311.22933	320.87989
	Sample 2	–1.392605	83.701254	1.000	–317.44721	314.66200
	Sample 3	9.368279	83.701254	1.000	–306.68633	325.42289
	Sample 4	1.617628	83.701254	1.000	–314.43698	317.67224
	Sample 5	12.359558	83.701254	1.000	–303.69505	328.41417
	Sample 7	64.861209	83.701254	0.999	–251.19340	380.91582
Sample 8	Sample 1	–68.509628	83.701254	0.999	–384.56424	247.54498
	Sample 2	–74.727512	83.701254	0.997	–390.78212	241.32710
	Sample 3	–63.966628	83.701254	0.999	–380.02124	252.08798
	Sample 4	–71.717279	83.701254	0.998	–387.77189	244.33733
	Sample 5	–60.975349	83.701254	0.999	–377.02996	255.07926
	Sample 7	–8.473698	83.701254	1.000	–324.52831	307.58091

Table 6 Tests of normality.

	Kolmogorov-Smirnov			Shapiro-Wilk		
Samples	Statistic	*df*	Significance	Statistic	*df*	Significance
Sample 1	0.407	43	0.000	0.254	43	0.000
Sample 2	0.416	43	0.000	0.207	43	0.000
Sample 3	0.406	43	0.000	0.269	43	0.000
Sample 4	0.411	43	0.000	0.241	43	0.000
Sample 5	0.398	43	0.000	0.266	43	0.000
Sample 6	0.401	43	0.000	0.254	43	0.000
Sample 7	0.406	43	0.000	0.412	43	0.000
Sample 8	0.395	43	0.000	0.448	43	0.000

Table 7 Kruskal-Wallis test.

Chi-square	1.660
df	7
Asymptotic significance	0.976

https://doi.org/10.1017/RDC.2016.40 Published online by Cambridge University Press

Table 8 Mann-Whitney test.

Mann-Whitney *U*	840.500
Wilcoxon *W*	1786.500
Z value	–0.726
Asymptotic significance (2-tailed)	0.468

In addition, the Mann-Whitney test in Table 8 at $\alpha = 0.05$, which was used to compare Samples 6 and 8 to each other, shows also no significant difference between the samples. All these statistical data support the previous examination results and indicate that it is very likely that the source of the scoria Samples 6 and 8 collected from the fallen dome of the West Church is Quais volcanic cone.

CONCLUSIONS

The West Church at the Umm el-Jimal archaeological site was built with basalt stones widespread in the area surrounding the site, while large fragments of scoria were used for the production of lightweight concrete used for its dome. Although the ^{14}C dating of the dome to the 4th century AD does not agree with the suggested archaeological dates, the ^{14}C date is possible because Umm el-Jimal belonged to the Bosra Bishopric, which is not far from Umm el-Jimal, and was one of the important religious capitals and a center for the episcopal chair. In addition, Umm el-Jimal comprises Julianos church, another church of the same date. The closest source of scoria to Umm el-Jimal is the Quais volcanic cone and the similarities of macroscopic, microscopic, mineralogical, and chemical composition of the scoria samples of the dome compared to the Quais volcanic cone strongly suggest that the probable source of the scoria is the Quais volcanic cone.

ACKNOWLEDGMENTS

This work was made possible by a grant from the deanship of scientific research and higher studies at Yarmouk University. The author would like to acknowledge the Department of Antiquities, Jordan, for the permission to collect samples and Dr Abdul Qader Al-Housan for his comments and help in collecting the samples. I would like to thank Dr Adel Al-Widyan for his help in the statistical analyses.

REFERENCES

Al-Bashaireh K. 2014. Reconstructing the chronology of the house XVII–XVIII complex at Umm el-Jimal, east Jordan: radiocarbon dates of organic inclusions of architectural mortars. *Radiocarbon* 56(1):245–56.

Al-Malabeh A. 1993. The volcanology, mineralogy and geochemistry of selected pyroclastic cones from NE-Jordan and their evaluation for possible industrial applications [unpublished PhD thesis]. Erlangen: Erlangen University.

Bender F. 1974. *Geology of Jordan*. Berlin: Gebrüder Bornträger.

Bowman SH. 1990. *Radiocarbon Dating*. Berkeley: University of California Press.

Bronk Ramsey C. 2009. Bayesian analysis of radiocarbon dates. *Radiocarbon* 51(1):337–60.

Bronk Ramsey C, Lee S. 2013. Recent and planned developments of the program OxCal. *Radiocarbon* 55(2–3):720–30.

Butler HC. 1913. *Ancient Architecture in Syria, Southern Syria: Umm Idj-Djmâl. Division II.* Leiden: Brill.

Camuti KS, McGuire PT. 1999. Preparation of polished thin sections from poorly consolidated regolith and sediment materials. *Sedimentary Geology* 128(1):171–8.

Chandra S, Berntsson L. 2002. *Lightweight Aggregate Concrete: Science, Technology and Applications.* New York: William Andrew Publishing.

De Vries B. 1990. *Umm el-Jimal: "Gem of the Black Desert": A Brief Guide to the Antiquities*. Amman: Al Kutba Publishers.

De Vries B. 1993. The Umm el-Jimal Project, 1981–1992. *Annual of the Department of Antiquities of Jordan* 37:433–60.

De Vries B. 1994. What's in a name: the anonymity of ancient Umm el-Jimal. *Biblical Archaeologist* 57(4):215–9.

De Vries B. 1998. *Umm el-Jimal: A Frontier Town and its Landscape in Northern Jordan.* Volume I. Journal of Roman Archaeology, Supplementary Series no. 26.

Dunn E, Rapp GR. 2004. Characterization of mortars and pozzolanic materials from Umm al-Jimal. *Studies in Conservation* 49(3):145–60.

Duran A, Robador MD, Jimenez de Haro MC, Ramirez Valle V. 2008. Study by thermal analysis of mortars belonging to wall paintings corresponding to some historical buildings of Sevillian art. *Journal of Thermal Analyses and Calorimetry* 92(1):353–9.

Harries KA. 1995. Concrete construction in Early Rome. *Concrete International* 17(1):58–62.

Hossain KMA. 2006. Blended cement and lightweight concrete using scoria: mix design, strength, durability and heat insulation characteristics. *International Journal of Physical Sciences* 1(1):5–16.

Jull AJT, Burr GS, McHargue LR, Lange TE, Lifton NA, Beck JW, Donahue DJ. 2004. New frontiers in dating of geological, paleoclimatic and anthropological applications using accelerator mass spectrometric measurements of ^{14}C and ^{10}Be in diverse samples. *Global and Planetary Change* 41(3–4):309–23.

Kogel JE, editor. 2006. *Industrial Minerals and Rocks: Commodities, Markets, and Uses*. Colorado: Society for Mining, Metallurgy and Exploration.

Kwon JS, Yun ST, Lee JH, Kim SO, Jo HY. 2010. Removal of divalent heavy metals (Cd, Cu, Pb, and Zn) and arsenic (III) from aqueous solutions using scoria: kinetics and equilibria of sorption. *Journal of Hazardous Materials* 174(1):307–13.

Lancaster L. 2011. The use of lightweight concrete in Rome, Cilicia, and Tunisia. In: Ringbom Å, Hohlfelder RL, editors. *Building Roma Aeterna*. Current Research on Roman Mortar and Concrete. *Commentationes Humanarum Litterarum* 128:60–72.

Lancaster L, Sottili G, Marra F, Ventura G. 2010. Provenancing of lightweight volcanic stones used in ancient Roman concrete vaulting: evidence from Turkey and Tunisia. *Archaeometry* 52(6): 949–61.

Lancaster L, Sottili G, Marra F, Ventura G. 2011. Provenancing of lightweight volcanic stones used in ancient Roman concrete vaulting: evidence from Rome. *Archaeometry* 53(4):707–27.

Lechtman HN, Hobbs HW. 1987. Roman concrete and the Roman architectural revolution. In: Kingery WD, editor. *Ceramics and Civilization Volume 3*. Westerville, Ohio: American Ceramic Society. p 81–128.

Moropoulou A, Bakolas A, Bisbikou K. 1995. Characterization of ancient Byzantine and later historic mortars by thermal and diffraction techniques. *Termochimica Acta* 269:779–95.

Moropoulou A, Bakolas A, Bisbikou K. 2000. Investigation of the technology of historic mortars. *Journal of Cultural Heritage* 1(1):45–58.

Moropoulou A, Bakolas A, Aggelakopoulou E. 2004. Evaluation of pozzolanic activity of natural and artificial pozzolans by thermal analysis. *Termochimica Acta* 420:135–40.

Piccirillo M. 1981. *Chiese e mosaici della Giordania settentrionale*. Jerusalem: Franciscan Printing Press.

Reimer PJ, Bard E, Bayliss A, Beck JW, Blackwell PG, Bronk Ramsey C, Buck CE, Cheng H, Edwards RL, Friedrich M, Grootes PM, Guilderson TP, Haflidason H, Hajdas I, Hatté C, Heaton TJ, Hoffmann DL, Hogg AG, Hughen KA, Kaiser KF, Kromer B, Manning SW, Niu M, Reimer RW, Richards DA, Scott EM, Southon JR, Staff RA, Turney CSM, van der Plicht J. 2013. IntCal13 and Marine13 radiocarbon age calibration curves 0–50,000 years cal BP. *Radiocarbon* 55(4):1869–87.

Sebestyén G. 1998. *Construction: Craft to Industry*. New York: Routledge.

Stefanidou M, Papayianni I. 2005. The role of aggregates on the structure and properties of lime mortar. *Cement and Concrete Research* 27: 914–9.

Sweet SA, Grace-Martin KA. 2012. *Data Analysis with SPSS: A First Course in Applied Statistics*. 4th edition. New York: Pearson Education.

Watson P. 2001. The Byzantine period. In: MacDonald B, Adams R, Bienkowski P, editors. *The Archaeology of Jordan*. Sheffield: Sheffield Academic Press. p 546–602.